No.13 Journal of Petroleum Research & Studies (JPR&S)

A Comparison of Soybean Oil Methyl Ester and Diesel Sprays behavior and atomization characteristics

Ahmad K. Jassim*; Basim A. Abd Alhay; Rakad K. Abd Al Kadhim; Fatima Kh. Hato; Dhaa A. Hashim

Petroleum Engineering Department, College of Engineering, University of Basra,

Abstract:

The present numerical study compares between spray characteristics of diesel and soybean oil methyl ester (SME biodiesel) under non-evaporating sprays. The spray structure of diesel and biodiesel fuel (soybean oil) in a common rail injection system are investigated and compared with that of available experimental data used image processing and atomization performance analysis. The proposed approach for the liquid phase based on the statistical properties of sprays be used to describe the liquid and gas phases in an Eulerian-Eulerian approach. The main concept for this model is the possibility of describing a poly disperse spray by using moments of a drop number size distribution function. The main reason for less spray tip penetration in

the (SME) comparing with diesel because a larger droplet diameters is the higher density, viscosity and surface tension of (SME). The effect of fuel properties on the near nozzle structure is studied. The comparisons are referring that the spray drag, breakup and collision processes are promoted.

Keywords:

Spray modeling, biodiesel spray, spray structure, Drop number size moments

1.Introduction:

Environmental interest and energy conservation have become crucial issues in industrial and automotive fields. Therefore alternative fuel resources are being passively researched as part of an effort to reduce the side effects of emissions and environmental problems. The common understanding of the necessity to use a clean, biodegradable and renewable fuel as alternative fuel has led to present the biodiesel as outstanding solution for the energy security and environment problems. During the last two decades, a big effort has been spent on the effect of alternative fuel properties. In the same way, biodiesel can improve the thermal efficiency through the optimum combustion process and reduced exhaust emission characteristics of diesel engine which is affected by fuel properties and spray atomization characteristics. Applicative research based on using different biofuels expressed that the fuel with higher density, viscosity and surface tension gives shorter spray tip penetration and large cone angle [1-5].

Experimental and numerical work have been carried out by Park et al. [6] to study the spray and atomization characteristics of an undiluted biodiesel fuel. They used a visualization system to analyses spray tip penetration, spray area and centroid variations while the droplet size and droplet distribution was obtained using a droplet measuring system. The numerical part had been implemented by using KIVA-3V code. They found when the injection pressure increases the injection delay decreased because of the increase of spray fuel b y injection pressure.

Majhool and ALJeebori .[7] studied numerically the modelling of spray of biodiesel in terms of spray moment framework. In their investigations were conducted for biodiesel spray under transient engine conditions. The spray tip penetration of biodiesel had been studied in a comparison with diesel fuel in a diesel engine under transient engine conditions. The predicted results were compared with experimental data with a chosen case for highly ambient pressure. The study used the Eulerian-Eulerian approach for the two phase flow simulation. In the validated computer programme both used liquid fuels are treated in terms of spray moments of drop size distribution. One parameter was chosen for the analysis and to study the spray characteristics through the examination and tracking the behaviour of the biodiesel.

2. Method

2.1. Moments theory

Beck and Watkins [8] presented their approach based on the droplet number size distribution, n(r), is defined as a multiple of the droplet number probability distribution of droplet radius as below

$$n(r) = \int_{r_{min}}^{r_{max}} N(r)\mathrm{d}r \qquad (1)$$

where N (r) is the droplet number probability distribution. The integral over all droplets provides the total number of droplets per unit total volume (not unit liquid volume). This can be defined as below:

$$Q_0 = \int_0^{\infty} n(r)\mathrm{d}r \qquad (2)$$

This is the first moment of the distribution function. In this approach, the three remaining distribution function moments are defined as below:

$$Q_i = \int_0^{\infty} r^i\, n(r)\mathrm{d}r \qquad (3)$$

At a particular point in space and time, Q0,is the total number of drops present, Q1, is the total sum of radii of the drops, 4πQ2, is the total surface area of the drops and 4πQ3/3 is the total volume of the drops, all quantities within a unit volume of the gas/liquid mixture. The fourth moment is related to the liquid volume fraction via the following relation

$$\frac{V_{liquid}}{V_{liquid}+V_{gas}}=\frac{4\pi}{3}Q_3=1-\Theta \qquad (4)$$

where Θ is the gas volume fraction. Furthermore, these four parameters provide all mean droplet diameters from D10 to the Sauter mean diameter D32, as, by definition

$$D_{pq}^{p-q}=\frac{2^{p-q}Q_p}{Q_q} \qquad (5)$$

3. Gamma distribution

The general gamma number size distribution is given by

$$n(r)=Q_0\frac{(k+2)^k}{\Gamma(k)r_{32}}r^{k-1}e^{-(k+2)\frac{r}{r_{32}}} \qquad (6)$$

and

$$\Gamma(k)=\int_0^\infty x^{k-1}e^{-x}dx \qquad (7)$$

where Γ(k) is the gamma function and r32 is the Sauter mean radius of the number size distribution of the drops. This is defined by r 32 = Q3/Q2. For numerical calculations, the gamma function can be approximated by [9]:

$$\Gamma(k)=((\frac{k}{e}(k*sinh(\frac{1}{k}+\frac{1}{810k^6}))^{1/2})^k)(\frac{2\pi}{k})^{1/2} \qquad (8)$$

with an error of at most 1% for values of k > 1.0. With three moments calculated through transport equations, there are two parameters (Q3/Q2 =r32)and (Q2/Q1) available to determine r32and k. Insertion of (18) into (2)and partial integration leads to

$$Q_i = \frac{(k+2)Q_{i+1}}{(k+i)r_{32}} \tag{9}$$

hence, setting i = 1,

$$k = \frac{2Q_r - 1}{Q_r - 1} \tag{10}$$

and

$$Q_r = \frac{Q_2^2}{Q_1 Q_3} \tag{11}$$

Q0 is calculated from equation(21), by setting i = 0. The gamma distribution is defined for all k > 0. However, in practice there are a number of restrictions that must be applied, arising from the sub-models employed; in particular, the drag model break-up and collision models used. The sub-models are derived in details in [10].

3.1. Transport equations

The convection velocity required is thus seen to be the expected moment average value (denoted by subscript 3), and the equation clearly represents a liquid-phase continuity equation. The source term has only one contribution due to evaporation, as the other phenomena considered do not affect the total mass of liquid present. The equations for the

remaining moments take a similar form, but more care must be taken as more source terms arise due to the changes effected by droplet breakup, droplet - droplet collisions, evaporation and changes in the droplet density. The equations are

$$\frac{\partial}{\partial t}(Q_i) + \frac{\partial}{\partial x}(Q_i U_{lij}) = -S_{Q_i} \qquad (12)$$

Use of the i -th moment-average velocity in the equation should be noted. The liquid mass-average velocity, or liquid momentum equation, as employed in the calculation scheme, is based on the work of Harlow and Amsden [11] for particulate flows. Equation is derived starting from the Lagrangian form of the equation for a group of droplets with identical properties, and the details of derivation of this equation appeared in Beck and Watkins [12]. In brief, the liquid phase momentum equation is written as

$$\frac{\partial}{\partial t}(\rho_l(1-\Theta)U_{l3i}) + \frac{\partial}{\partial x_j}(\rho_l(1-\Theta)U_{l3i}U_{l3j}) + U_{l3i}S_m = \frac{\partial}{\partial x_j}(\rho_l(1-\Theta)\sigma_v\nu_l(\frac{\partial U_{l3i}}{\partial x_j} + \frac{\partial U_{l3j}}{\partial x_i})) - S_{U_i} \qquad (13)$$

where σv is the coefficient of Melville and Bray [12], vl is the turbulent equivalent viscosity, Sm and S Ui are the source terms of mass and momentum, respectively. The remaining equations for the moment-average velocity are derived in a similar manner as described by Beck and Watkins [12].

4. Test case

According to the experiments of Kim et al. [13] the non-reactive diesel spray is tested in a constant volume combustion chamber. Droplet sizes and velocities are measured using Particle Doppler Analyser instrumentation. The injection pressure starts at 50 MPa and varies with needle position in nozzle. The trapped pressure is 0.1 MPa and the nozzle diameter is 0.3 mm. This tests is carried out for different initial gas phase pressures but one case here is adopted as

shown in table 1 where the initial gas temperature is 293 K. Table 2 shows adopted biodiesel properties which are given by Kim et al.[13].

5. The complete algorithm

The solution algorithm is based on the PISO algorithm of Issa [14], with the liquid phase equations added into it. The PISO algorithm provides an efficient non-iterative solution procedure that couples the gas-phase pressure and velocity components by an operator splitting technique and solves the equations of motion for the gas phase in a predictor corrector fashion. The current scheme solves the liquid equations only once, at the beginning of the time step. The use of a non-iterative scheme implies that some effects are lagged, i.e. carried forward from one time step into the next. In the current approach, the source term due to the drag effect is calculated at the end of the time step. The solution proceeds in the following manner at each time step:

• Step 1. The gas phase velocity components are predicted using the gas phase momentum equations.

• Step 2. The first set of pressure correction equations are solved (see Issa, [14] for details), as are the gas phase transport equations for energy Eg and vapour mass fraction f. The gas phase pressures, densities and velocity components are corrected.

• Step 3. The second set of pressure correction equations is solved. The gas phase pressures, densities and velocity components are corrected again.

• Step 4. Transport equations are solved for the turbulence kinetic energy and its dissipation rate. The equations are coupled and iterated to convergence. The turbulent viscosity is recalculated.

• Step 5. The transport equations for the moment-average liquid velocities, Ul1, Ul2

and Ul3 , are solved.

• Step 6. The inter-phase drag, breakup and collision source terms are evaluated.

• Step 7. The transport equations for the moments Q1, Q2and Q3of the drop size distribution and for the liquid are solved. The void fraction is updated.

6. Results and discussions

Before considering the computational results extracting from the in-house code written in FORTRAN-2003. The code is able to read structured or unstructured grid created by GAMBIT with neutral extension. GAMBIT software is used for supplying strategy for increasing grid refinement based on enlarge grid resolution at certain places by increase the number of intervals or the compression ratio. Figure (1) shows the computational domain used in this simulation. Here the objective of the refinement of grids can be used to capture flow details without being excessive as determined by non-zero droplets source terms in a grid cell. The details of the specified computational domain are: (No. volumes 1906), (No. Faces 3901), (No. vertices 1996) and (No. injection cells 5).

The diesel and biodiesel spray structure elements which are investigated in this study include spray tip penetration, spray velocity (both components axial and radial) and spray Sauter mean diameter. The validation of the proposed numerical solution is discussed in this section. The simulation results are compared with the experimental available results for the biodiesel Soybean Oil Methyl Ester (SME) have been taken from the literature presented by Kim et al. [13].

Spray tip penetration has been analyzed according to the comparison with available experimental data by Kim et al. [13]. Spray tip penetration is defined as maximum length achieved by the spray droplets during the injection period. The ambient pressure was kept constant at 0.1MPa for the test case. Spray tip penetrations btained from the experiment were measured either by Phase Doppler Anemometry (PDA) or photographically. For the calculations it is determined as the axial position behind which 90% of the liquid volumes are contained. Included are most of the relative interactions between spray droplets and ambient gas as modeled in spray sub-models Figure (2) shows predicted spray tip penetration in comparison with experimental data. The results show the agreement between simulation and experimental data is very satisfactory. According to this figure, time-dependent development

of the spray tip penetration length can be divided into two intervals. The first time interval starts at the beginning of injection (t = 0 msec) when the needle begins to open and ends at the moment the liquid droplets emerging from the nozzle hole begin to disintegrate (here until t =1 msec). The simulated results are over predicted as compared with the experimental data because of the small needle lift and the low mass flow rate at the beginning of injection. This leads the injection velocity is small. During the second interval (t >1 msec), the spray tip penetration simulated results presented the good consistent with the experimental results. The reason is the spray tip velocity is approximately close to the experimental velocity during the second period.

Now the aim of this study will start by comparing three mainly parameters to characterized Soybean Oil Methyl Ester (SME). Firstly, Figure (3) shows the liquid volume faction at time 2 msec. To figure out the distribution of the liquid volume fraction, the axial direction was chosen to illustrate the way in which the liquid droplets are spread out. From this contour plot the liquid volume or concentration increases near the injector due to the liquid mass has been injected for 1.2 msec. whereas it can be noticed that at the front of the spray as the less concentration is found because it is associated with the atomization processes. The liquid volume fraction in diesel exhibited more penetration and wide cone angle than the (SME). This is because, the most important reason described here in this work is the fuel physical properties. For example the fuel density can be affected on the atomization process and spray tip penetration by decelerating the injection delay time as will be presented below.

$$U_{inj} = cd\sqrt{\frac{2(P_{inj} - P_{amb})}{\rho_{liq}}} \qquad (14)$$

Figure (4) shows contour plot for a comparison between diesel and (SME) at time 2.0 msec. After the start of injection of liquid, the smaller droplets were seen to move towards the Centre of spray because of the entrained gas velocity induced by the spray. Also the Sauter mean

diameter can be defined as (SMD=Q3/Q2). That explain the highest values can be found at the axis of symmetry.

In order to achieve as good comparison as possible with the data, the inlet conditions were matched as closely as possible to the data given by Kim et al [14]. In particular, the variation of injection pressure with time was overcome by using the injection pressure profile to minimize the error of a few percent by using the injection profile. In the first 0.2 ms the injection pressure rises linearly with time from an initial value of 40 MPa to its maximum value of 50 MPa. As a consequence the computed injection velocity follows similar trends. injection. A constant value of discharge coefficient was set at 0.7.

Figure (5) shows a comparison between the predicted of the liquid velocity components after 2.0 ms for the diesel and (SME) liquid fuels. The third moment velocity components are used for this comparison, as they are closer in nature than area and drop radii-averaged velocities. The axial profile shows that the maximum velocity occurs at the core of the spray (at the axis of symmetry). That is because large droplets which are heaviest (biggest momentum) are found here.

7. Conclusions

The aim of this study is to perform an optimal numerical simulation for biodiesel spray in a common rail diesel engine. As is apparent from methods of computational, the advanced numerical techniques can perform well as compared with the experimental data. The conclusions that are obtained by this work are as follows:

1. The spray tip penetration simulated results presented the good consistent with the experimental results. The liquid volume fraction and surface area concepts (based on spray moment theory) can cope with interactions between the two-phases with less computational effort and more efficiently.

2. One of the main advantages to use the numerical simulation will be appeared here. The computational calculations can provide the comparison with the experiment by adding the range of droplet sizes.

References

1. S. Lee, D. Tanaka, J. Kusaka, and Y. Daisho. Effects of diesel fuel characteristics on spray and combustion in a diesel engine; JSAE200224660, Japanese Society of Automotive Engineers: Tokyo, Japan, 2002.

2. C. S. Lee, S.W.Park, and S. I. Kwon. An Experimental Study on the Atomization and Combustion Characteristics of Biodiesel-Blended Fuels. Energy Fuels,19 (2005), 2201.

3. Y. Wengiao. Computational modelling of nitrogen oxide Emissions from biodiesel based on accurate fuel properties. W. Yuan, PhD Dissertation, University of Illinois at Urbana Champaign. Department of Agricultural and Biological Engineering, 2006.

4. C. A. W. Allen. Prediction of biodiesel fuel atomization characteristics based on measured properties. PhD Dissertation, Dalhousie University DALTECH, Halifax, Canada, 1998.

5. K. Yamane, A. Ueta, and Y. Shimamoto. Influence of Physical and Chemical Properties of Biodiesel Fuel on Injection, Combustion and Exhaust Emission Characteristics in a DI-CI Engine, The Fifth International Symposium on Diagnostics and Modeling of Combustion in IC Engines COMODIA, Nagoya, Japan, July 14, 2001.

6. Su Han Park, Hyung Jun Kim, Hyun Kyu Suh and Chang Sik Lee. A study on the fuel injection and atomization characteristics of soybean oil methyl ester (SME). International Journal of Heat and Fluid Flow,30 (2009), 108–116.

7. Ahmed Abed Al-Kadhem Majhool and Abbas Alwi Sakhir ALJeebori. Study of modelling spray penetration of biodiesel fuel under transient engine conditions. Academic Research International. Vol. 3, No. 3, November 2012, 70–79.

8. J. C. Beck and A. P. Watkins. On the development of a spray model based on drop-size moments. Proc. R. Soc. Lond., A(459)(2003),1365-1394.

9. R.H. Windschitl, http://www.rskey.org/gamma.htm.

10. J. C. Beck and A. P. Watkins:On the Development of Spray Submodels Based on Droplet Size Moments. Journal of Computational Physics 182, 586621,2002.

11. F.H. Harlow, and A. A. Amsden: Numerical calculation of multiphase fluid flow. Journal of Computational Physics, 17, 19–52, 1975.

12. J. C. Beck and A. P. Watkins. On the development of a spray model based on drop-size moments. Proc. R. Soc. Lond., A(459):13651394,2003a.

13. Hyung Jun Kim, Su Han Park and Chang Sik Lee. A study on the macroscopic spray behavior and atomization characteristics of biodiesel and dimethyl ether sprays under increased ambient pressure. Fuel Processing Technology 91 (2010) 354363

14. R. I. Issa. Solution of the implicitly discretised fluid flow equations by operator splitting. Journal of Computational Physics, 61, 40– 65, 1986.

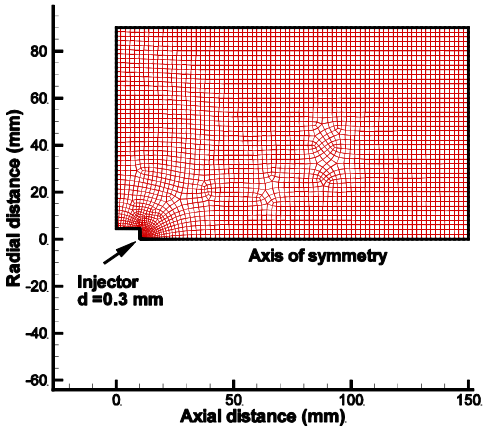

Fig.(1) Computational domain

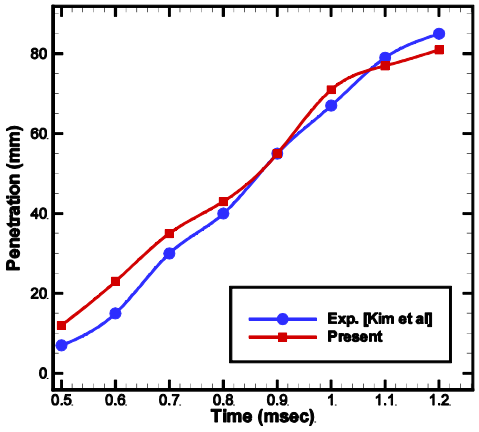

Fig.(2) Spray penetration

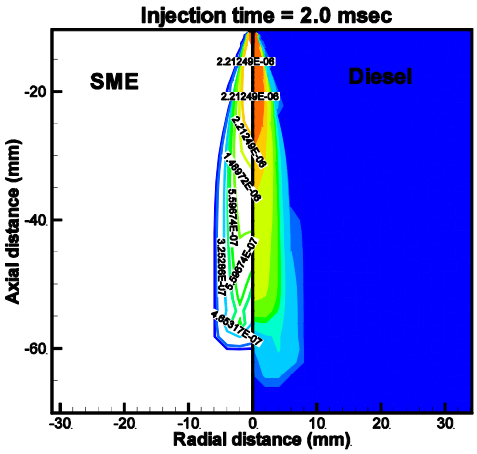

Fig.(3)Liquid volume fraction

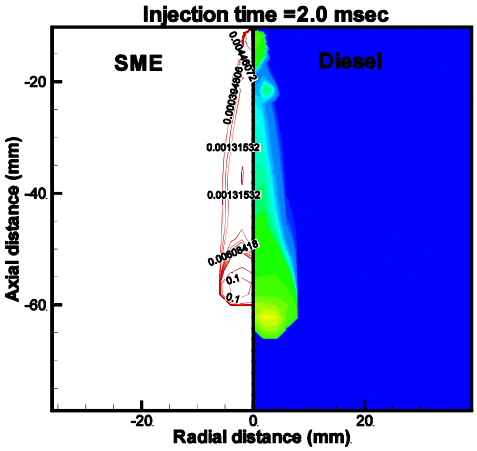

Fig. (4) Sauter mean diameter

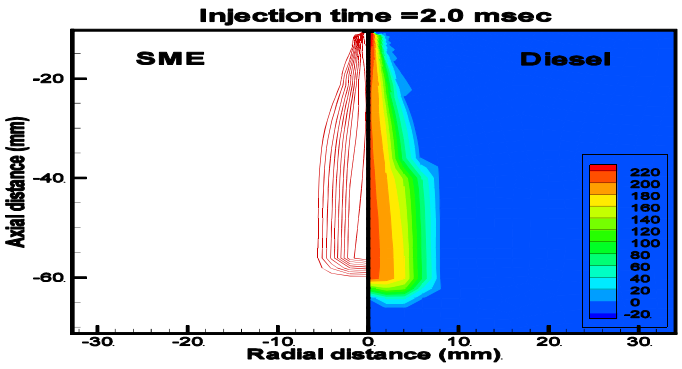

Fig. (5)Spray axial velocity

Table 1: Physical conditions for the parametric tests and experimental validations (Data of Kim et al. [13].)

	Kim et al
Injection system–	*Common–rail*
Fuel Type–	*Biodiesel*
Nozzle Type–	$Mini-sac$
Number of nozzel holes–	*Single hole*
Injection Pressure (MPa)	50.0
Nozzle Radius (mm)	0.3
Chamber Length (mm)	100.0
Chamber Radius (mm)	20.0
Injection SMR (μm)	25.0
Time Step (μsec)	2.0
Injection duration ($msec$)	1.2
Temperature of Gas (K)	293
Gas Pressure (MPa)	0.10
Gas Density (kg/m^3)	13.8

Table 2: Properties of biodiesel (Data of Kim et al. [13].)

	$Kim1$
Density kg/m^3	884
Viscosity mm^2/sec	$4.0-6.0$
Surface tensionkg/sec^2	0.028
Boiling point temperature$K$	$588-623$
Flash point temperature K	$373-443$
Cetane number –	$48-65$